Earthquake Engineering, Tenth World Conference © 1992 Balkema, Rotterdam. ISBN 90 5410 060 5

Cyclic post-elastic behavior of critical regions of R.C. beam-column joints

S. Albanesi & S. Biondi
Institute of Civil Engineering, University of Ancona, Italy

ABSTRACT: An original global model, developed for the numerical analysis of monotonic and cyclic response of R. C. beams, has been employed to examine and control the most important phenomena that occur during post-elastic stress: some interesting and meaningful conclusions, based on an extensive numerical analysis, have been obtained.

1. INTRODUCTION

A good design of reinforced concrete frames, subjected to seismic loading, requires the modelling of ductile behavior of critical regions of beams, where the post-elastic phenomena occur.

In order to obtain a good flexural response of the beam, at the beam-column joint, many conditions have to be investigated and controlled. An original global model, which the Authors have been developing in a computer program since 1988 and upgraded for the last time in 1991, can simulate and take into account with good accuracy the most important mechanisms occurring during post-elastic stress, both in monotonic and cyclic loading. Various models, each describing one or more mechanical and structural events, are combined into a general implementation.

It is therefore possible to investigate a r. c. element subjected to a prescribed section deformation history; the model can evaluate and control, step-by-step, the structural degradation and can predict the type of failure which will occur and the general behavior during post-elastic response.

Comparison with many experimental results exhibits a good accordance and, moreover, the mathematical model allows to isolate the structural degrading conditions which cannot be appreciated in experimental tests, as some of them often occur suddenly and nearly at the same time.

In this paper the above model is summarized and some results are discussed, concerning comparison between monotonic and cyclic behavior and quality of response. The aim of the research is to determine design criteria in order to obtain the optimal response in terms of ductility level; therefore, although the model can control some fragile events and other conditions, the attention is directed to some specific cases where these events are avoided. Consequently, only responses of ductile geometric and mechanical cases are presented, i.e. with deep rectangular beams and good anchorage of the reinforcing bars in interior beam-column joint.

2. GLOBAL MODEL FOR NUMERICAL ANALYSIS

The analysis performed by the above-mentioned computer program proceeds in the following way: a curvature is assigned to the most critical section in accordance to a prescribed loading history; equilibrium is determined for each homogeneous portion of the beam and the structural status of the whole is hence controlled; the procedure is iterated until a conventional failure occurs.

The beam is divided into subregions each with constant geometrical and mechanical characteristics; a layered model is used for the cross section in order to consider separately the unconfined concrete, the core and the reinforcing bars. These layers are allowed to strecth and contract axially under flexure, the longitudinal strain in steel and concrete is assumed to be directly proportional to the distance from the neutral axis.

This approach permits to calculate the flexural quota of the global response, by using the constitutive laws described below.

The fixed end rotation, due to bars slipping in the joint, is investigated by means of an original finite element method. Two kinds of spring elements are introduced: the first are arranged in series connection and model a bar portion subjected to axial force, while the second, arranged in parallel and rigidly constrained at one end, model the bond-slip mechanism.

2.1. Constitutive laws

The modified Kent-Park model is assumed in order to describe concrete behavior, in tension and in compression, both confined and unconfined. According to this model, monotonic envelope and cyclic branches are defined, step by step, with regard to the geometry of the cross section, the amount of transversal reinforcement and the distribution of internal stresses.

For cyclic loading, linear relationships between the point where unloading begins and the one which corresponds to zero stress are considered.

The monotonic stress-strain curve of steel is a cubic hardening strain one and presents three regions: the first exhibits an elastic behavior (E_s) up to ε_{sy} and f_y; the second is perfectly plastic for strains below ε_{sh}; the third, which begins with slope E_{sh}, is defined by:

$$\sigma_s = a\, e^3 + b\, e^2 + E_{sh}\, e + f_y$$

where $a = E_{sh} / e_u^{0.5} - 2\,(f_t - f_y)\, e^{-1/3}$

$b = [3\,(f_t - f_y) - 2\,E_{sh}\, e_u]\, e_u^{-0.5}$

$e = \varepsilon_s - \varepsilon_{sh}$, $e_u = \varepsilon_{su} - \varepsilon_{sh}$

and terminates at the point (ε_{su}, f_t), with zero slope. In the strain-hardening range ($\varepsilon_{sh} \le \varepsilon_s \le \varepsilon_{su}$) the condition $[1.5\,(f_t - f_y)/e_u \le E_{sh} \le 3\,(f_t - f_y)/e_u]$ must be satisfied.

The cyclic behavior of steel, in accordance to the Pinto-Menegotto model, is asymptotically contained within the monotonic curves which are defined in connection with strain development; failure depends on tensile or compressive strain.

Particular attention is given to the instability of reinforcing bars, which determines loss of compressive stiffness, but preserves their tensile structural function; this phenomenon can occur both within stirrup spacing and between the crack faces, requiring respectively a different approach to failure modelling.

The bond-slip relationship is able to take account of the amount of energy dissipation along the bars, considering the local deterioration and the number and amplitude of hysteretic cycles; bond failure occurs when the slip in the joint exceeds an ultimate limit, which depends on geometric parameters. The bond-slip relationship is characterized at each step by means of an energy criterium.

Regarding slip u and bond tension q, the constitutive relationship, in accordance to Filippou et al., is defined through the parameters u_1, u_2, u_3, q_1, q_3, which depend on the materials and on the geometry of the anchorage; the monotonic law is defined in the following way:

for $u < u_1$ $\quad q = q_1\,(u/u_1)^{\alpha}$

for $u_1 \le u \le u_2$ $\quad q = q_1$

for $u_2 < u < u_3$ $\quad q = u\,(q_1 - q_3)/(u_2 - u_3) + (u_2\, q_3 - u_3\, q_1)/(u_2 - u_3)$

for $u \ge u_3$ $\quad q = q_3$

where α is a suitable parameter smaller than unity.

The cyclic behavior assumes a constant value for each of u_1, u_2 and u_3, while q_1 and q_3 are affected by reductive coefficients δ_i, depending on the total energy dissipation.

These parameters are assigned considering various situations, such as bar within confined or unconfined region of interior beam-column joint, bar in the beam with and without cover, bar in intermediate regions; in crossing from one region to another, suitable intermediate values of constitutive parameters are considered. The bond-slip problem is solved by prescribing optimized a priori conditions in the mid-point of the joint.

2.2. Finite element method for anchorage

In order to describe the response of reinforcing bars in the joint, the assumed model considers that these are subjected, at the nodal interface, to the forces deriving from the flexural analysis.

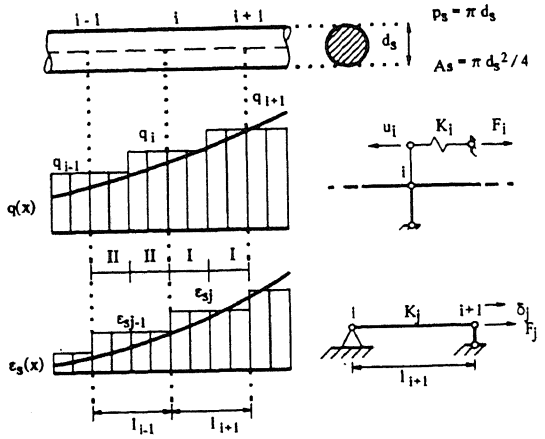

Figure 1.

As mentioned above, in accordance with fig. 1, the spring element j which models bars and the element i which simulates the bond-slip mechanism, have the following constitutive laws:

$F_j = K_j\, \delta_j$ $\qquad$ $F_i = K_i\, u_i$

where:

$F_j = \sigma_{sj}\, A_s$ $\qquad$ $F_i = 0.5\, q_i\, p_s\, (L_{i+1} + L_{i-1})$

$\delta_j = \varepsilon_{sj}\, L_{i+1}$

and K_i, K_j are the current values of stiffness ratio for spring elements.

Including all the forces F_j and F_i in the vector F and similarly δ_j and u_i in u, the problem is defined by:

$F = K\, u$

K is a three-diagonalized matrix.

The values of K_j and K_i depend on the stress history: while steel remains in the elastic range

$K_j = E_s\, A_s / L_{i+1}$

while, in general,

$K_i = 0.5\, K_u\, p_s\, (L_{i+1} + L_{i-1})$

where K_u, $[F\, L^{-3}]$, is the current tangent stiffness ratio in terms of q-u.

The solution of the problem is reached through the stiffness method, considering the forces at the extreme nodes to be known and hence determining the displacements.

The non linear nature of the problem has led to the constuction of an iterative procedure, which makes use of both the tangent and secant methods; this procedure is particularly useful when dealing with near-zero stiffness regions or softening branches.

The tangent method is applied in a small range in the vicinity of the solution, in order to avoid numerical instability and to refine the precision of the solution obtained through the secant method, applied in the first

phase of the procedure. The convergence of the tangent method is verified by checking that the succession $\{u_n\}$ of the displacements in the nodes of the bar $\{u\}$ is a non increasing bounded sequence with a final value "near enough" the solution.

In the application of the secant method, both residua of nodal forces and increments of displacements at all nodes must be less then a prefixed quantity, in order to guarantee the convergence of the next application of the tangent method.

When instability problems occur, the initial stiffness is employed, in order to define a pseudo-secant method.

A reinforcement bar reaches bond failure when the stresses applied at the ends cannot be equilibrated by bond along the bar.

The operator can choose a variable discretization step, depending on the structural geometry.

2.3. Failure conditions

Various structural conditions are detected by the global model procedure; all of the following can be taken into account:

- for top and bottom reinforcing bars: yielding, beginning of strain-hardening and failure at ultimate strain, all both in tension and in compression; buckling of bars with spalling off of cover within the stirrup spacing; buckling of bars between crack faces; occurrence of tensile stress with compressive strain and of compressive stress with tensile strain; all longitudinal reinforcing bars with tensile or compressive stress;
- for the concrete: tensile failure, crack closure, maximum compressive stress and perfectly plastic compressive strain, all both in top or in bottom cover and in upper side or in lower side of core; crack opening or crack closure in the entire section; ultimate compressive strain in upper side or in lower side of concrete core; spalling off of portions of top, bottom or lateral cover caused by exceeding ultimate compressive strain;
- for reinforced-concrete: spalling off of top or bottom cover caused by exceeding a characteristic value of compressive or tensile strain of bars; ultimate compressive strain in upper side or in lower side of concrete core and buckling of bars; bond failure of top or bottom bars in the joint.

The global model therefore considers the change in the section geometry due to crushing and spalling off of the top, bottom or lateral concrete cover, takes into account the presence of cracks at the joint interface and in a priori defined sections along the beam, evaluates the crack width through slipping of bars and plastic strain reached in concrete, and considers the effects of bent bars on flexural response and on cracking.

A parametric analysis for each load step is performed, in order to assess dangerous shear effects on cracks, which have to be avoided.

The conventional failure types, assumed as a stop condition for the numerical process, are:

a. failure at ultimate strain in tension in top or bottom bars;
b. failure at ultimate strain in compression in top or bottom bars;
c. buckling of top or bottom reinforcement bars between crack faces in order to avoid the consequent shear effects;
d. ultimate compressive strain in upper or lower side of concrete core and buckling of bars;
e. bond failure of top or bottom bars in the joint.

In a field of analysis set up within a range aiming to reach ductility, as that of the present research, only failure types a., d. and e. occur.

3. FIELD OF NUMERICAL EXPERIMENTATION

In this chapter the principal fields of investigation are summarized; part of an extensive program of numerical tests, performed by means of the global model, is presented.

3.1 Mechanical field

The present research deals with the following materials:

- concrete:	f_c = 25 MPa	f_{ct} = 2.5 MPa
	Ec = 25000 MPa	ε_o = 0.002
- steel:	f_y = 413 MPa	f_t = 517 MPa
	ε_{su} = 0.14	ε_{sh} = 0.00241
	E_s = 200000 MPa	E_{sh} = 2298 MPa

The type of steel considered, both for longitudinal and trasversal reinforcement, corresponds to FeB38K Italian reinforcement steel. In fact the input parameters are choosen to be as near as possible to the minimum mean values requested for acceptance of an industrial stock. The ratio between f_t and f_y is greater than 1.25, so this steel belongs to medium ductility class (DC"M") fixed by the Eurocode n° 8. In order to get closer to this code, the choice of input parameters is carried out so as to give a constitutive law to which corresponds, within the range $0 \le \varepsilon_s \le 0.01$, the same amount of energy as that given by the law $\varepsilon_s = \sigma_s/E_s + 0.823\,(\sigma_s/f_y - 0.70)^5$.

Furthermore the slope at the origin of the cubic function E_{sh}, is chosen such a way as to obtain a smooth cubic function.

It is therefore possible to define both E_{sh} and ε_{sh} in spite the Italian Code's not prescribing any suitable condition.

3.2 Geometric field

As mentioned above the beam is fixed to an interior beam-column joint, has a rectangular cross section with a 30 cm width and a 500 cm span between column interfaces; the layered model is made up of 15 layers for the lateral cover and of 60 layers for the concrete core.

Lacking reinforcement arrangements for relocated

plastic hinges, the length of these are conventionally set to $l_p = 0.50\ h + 0.125\ l' h^{-0.5}$ where l' is the shear span.

In the present numerical analysis the following main variation of parameters has been considered, in order to verify their influence on the amount of ductility:

- number of the reinforcement longitudinal bars, from 2 to 7, with diameter d_s = 14 and 16 mm;
- stirrup spacing Δ_{st}, equal to 5, 10 and 15 cm, with diameter d_{st} = 8 mm;
- height of the cross section equal to 50, 60 and 70 cm;
- embedment length, i. e. beam-column joint length, equal to 60 and 80 cm.

Considering all of these conditions, 216 different situations are tested both in monotonic and in cyclic range.

The prescribed embedment length, greater than 35 d_s, has the aim to obtain a good cyclic response in terms of anchorage.

The mimimun clear bar spacing, greater than d_s or 2 cm, avoids, in bond-slip mechanism, any negative effect due to stresses superimposition; therefore bond stress-slip relationships have in all cases the same parameters.

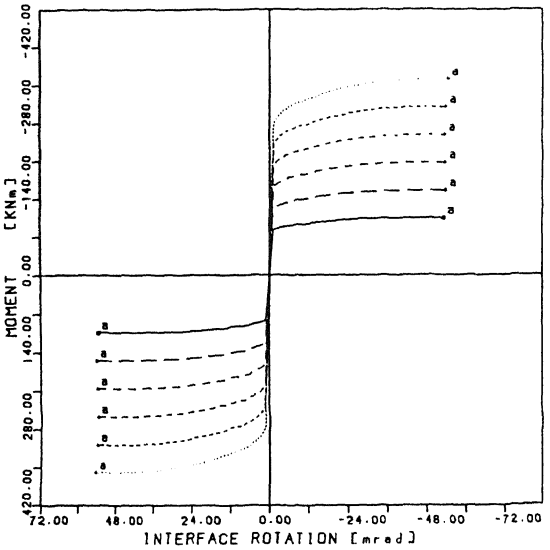

Figure 2.

3.3 Load field

The bending moment is expressed by a second degree law, which is composed by the curves due to vertical and seismic loads. The vertical loads are assumed as capable to stress the longitudinal reinforcement in tension up to a quarter of f_y.

These conditions permit to set the prescribed section deformation history for a cyclic test; this history has a mean value which corresponds to the vertical load curvature and is made of groups of three alternate loadings, increasing in value as a consequence of an input factor. Between each group a small cycle, in terms of prescribed deformation, is performed, in order to rearrange mechanical and mathematical phenomena.

The prescribed deformation step is therefore automatically rearranged with a suitable algorithm in order to reduce computer time and to avoid numerical instability; the increase of maximum deformation for each group of three cycles is set, in this paper, equal to one or three time the yielding value.

4. DISCUSSION ON SOME RESULTS OF MONOTONIC AND CYCLIC TESTS

To correctly interpret the diagrams, the following quantities are necessary:

$\theta_t = \theta_f + \theta_{fe}$

where:

θ_t = total interface rotation

θ_f = flexural rotation = $0.5\ l_p\ \phi_f$

θ_{fe} = fixed-end rotation.

This last one depends on crack depth, end slip of reinforcing bars and the position of the first core layer with zero crack width.

In fig. 2 the monotonic envelopes, both positive and negative, for 30x70 cm^2 beams with Ø14 reinforcing bars are presented. In this case all "a" failure conditions are registered; in fact these geometric situations are those with minimum reinforcement percentage.

In fig. 3 the situations with maximum reinforcement percentage are presented, i.e. 30x50 cm^2 beams with Ø16 reinforcing bars.

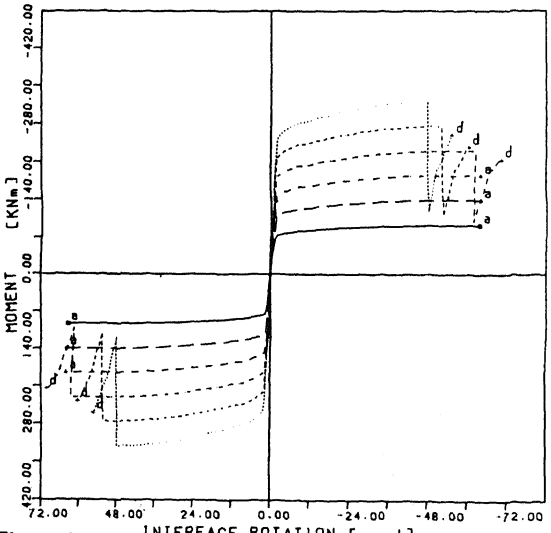

Figure 3.

In this case a reinforcement percentage exists for which the failure condition changes from "a" type, for low percentage, into "d" type.

With respect to all numerical data available the two

diagrams of fig. 4 are plotted, where:

ω_s = reinforcement percentage = $100\,(A_s^t + A_s^b)/A_c$

ω_{st} = transversal on longitudinal reinforcement ratio = $V_{st}/(A_s^t+A_s^b)\,\Delta_{st}$

μ_u = rotational ductility = θ_{tu}/θ_{ty}

μ_u^* = rotational ductility = $\theta_{tu}^*/\theta_{ty}$

and the apex * signifies a reinforcement instability situation.

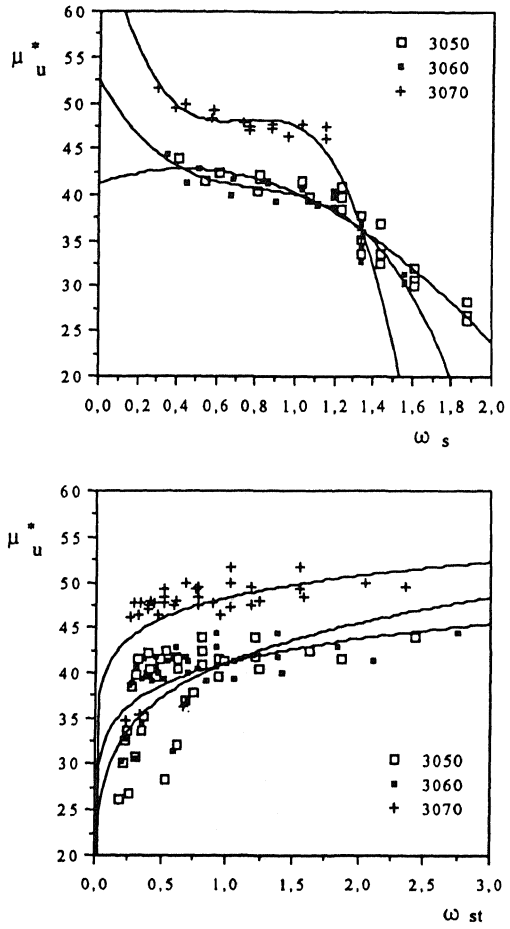

Figure 4.

The same path diagrams as those of fig. 4 are obtained considering the ductility μ_u.

It is possible to note that in the range of reinforcement percentage $\omega_s \approx 1.0 \div 1.4$ the ductility presents a strong decay; this phenomenon increases for greater reinforcement percentage. Moreover when ω_{st} is greater than ω_{st}^* increasing of ductility is very low and depends on concrete overstrength.

In fig. 5 beam overstrength, $\Phi_u = M_u^*/M_y$, for all considered geometries is plotted.

In this case it is possible to note a smooth variation in a small range of this parameter.

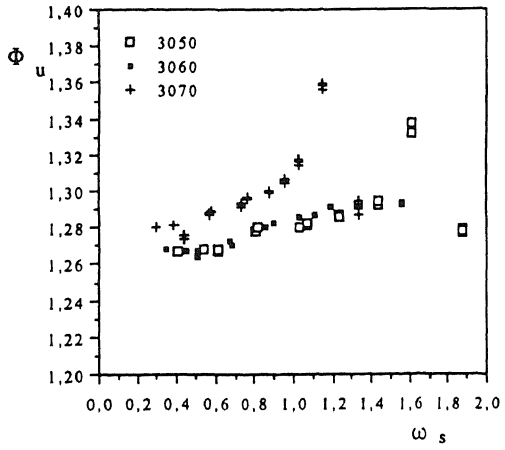

Figure 5.

No tested beam-column joints present, in monotonic range, an "e" failure type; this fact confirms a good anchorage design as above mentioned; still an important aspect of the problem remains to verify this anchorage effectiveness in the cyclic behavior.

As above mentioned, two kinds of cyclic deformation history are prescribed. In fig. 6 cyclic branches and monotonic envelopes, for a 30x50 cm^2 beam with 5+5 Ø16 and 80 cm anchorage length, are plotted.

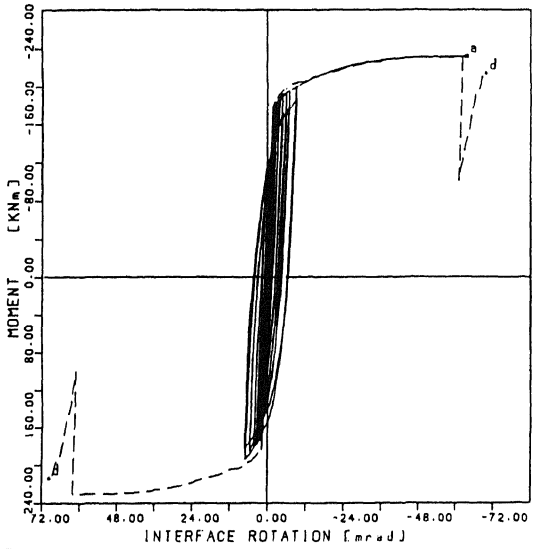

Figure 6.

In this case the range of cyclic deformation is not capable to cause an "e" type failure but only an "a" type instead of a "d" one with low, but appreciable, values of end slip and bond stiffeness in top reinforcing bars.

In fig. 7 cyclic branches for two 30x50 cm^2 beams with 60 cm anchorage are plotted; the first is that of a 7+7 Ø14 beam, the second that of a 5+5 Ø16 beam.

Both the situations shown in fig. 6 and the situations of fig. 7 are obtained with ω_s values as near as possible to the ω_s values of ductility decay for each beam. This choice is performed in order to investigate the connection between monotonic and cyclic behavior; with this in view the anchorage length is assumed equal to 60 cm.

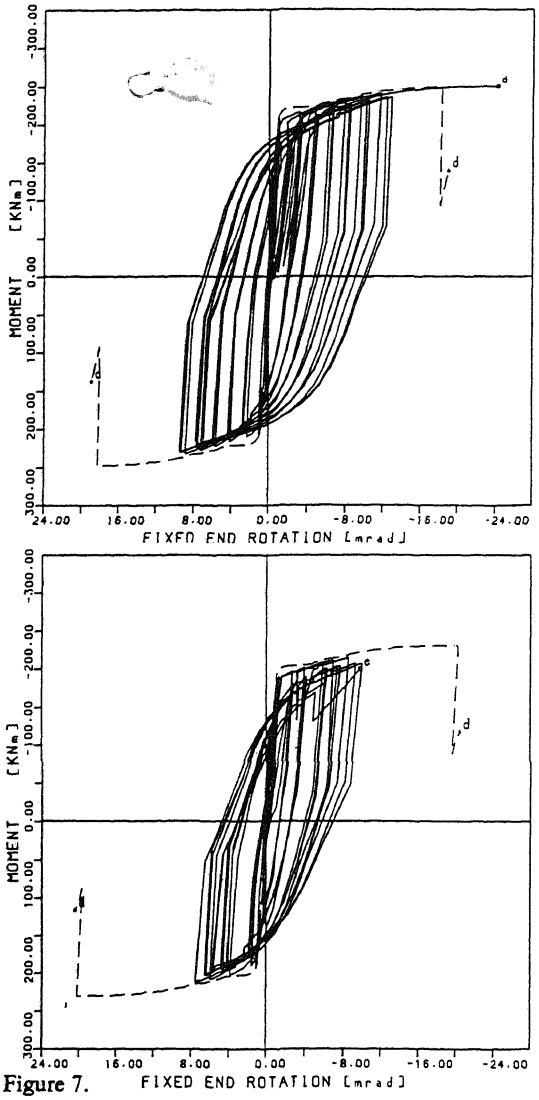

Figure 7.

In the cases of fig. 7 a great amount of end slip is evident; however in the first case, with the greatest reinforcement percentage, an "a" type failure is obtained whereas in the second the result is an "e" type one, caused by a greater value of reinforcing bar diameter, i.e. a greater decay of bonding along the joint anchorage.

These few cyclic cases seem to underline, for deep beams with low reinforcement percentage, that the ω_s value of ductility decay is also meaningful in terms of joint anchorage.

REFERENCES

Albanesi, S., Biondi, S. 1991. Ductility in cyclic post-elastic behavior of critical regions of R.C. beams near joints. *Proc. of the International Meeting on Earthquake Protection of Buildings:* 177/B-190/B. Ancona: C.R.E.A.

Ciampi, V., Eligehausen, R., Popov, E.P., Bertero, V.V. 1982. Analytical model for concrete anchorages of reinforcing bars under generalized excitations. *Rep. UCB/EERC* 82/23.

Cowell, A.D., Popov, E.P., Bertero, V.V. 1983. Effects of concrete types and loading conditions on local bond-slip relationships. *Rep. UCB/EERC* 83/17

Eligehausen, R., Popov, E.P., Bertero, V.V. 1983. Local bond stress-slip relationships of deformed bars under generalized excitations. *Rep. UCB/EERC* 83/23.

Filippou, F.C., Popov, E.P., Bertero, V.V. 1983. Effects of bond deterioration on hysteretic behavior of r. c. joints. *Rep. UCB/EERC* 83/19.

Giuriani, E., Gubana, A. 1988. Alternate plasticity of steel reinforcement in shear-wall under repeated loads. *Studi e Ricerche:* 263-274. Milano: Italcementi spa - Bergamo ed. 10.

Harajli, M.H., Mukaddam, M.A. 1988. Slip of steel bars in concrete joints under cyclic loading. *Journal of Structural Engineering* 114/9: 2017-2035.

Menegotto, M., Pinto, P.E. Method of analysis for cyclically loaded r.c. plane frames including changes in geometry and non-elastic behavior of elements under combined normal force and bending. *I.A.B.S.E. Symposium.* Lisbon: IABSE Report 13.

Russo, G., Zingone, G., Romano, F. 1990. Analytical solution for bond-slip of reinforcing bars in R.C. joints. *Journal of Structural Engineering.* 116: 336-355.

Soroushian, P., Obasaki, K., Marikunte, S. 1991. Pullout behavior of hooked bars in exterior beam-column connections. *Journal of Structural Engineering.* 117: 48-60.

Tada, T. 1987. Bond deterioration in reinforced concrete members subjected to seismic loading. *I.A.B.S.E. Colloquium:* 539-545. Deft: IABSE Report 54.

Tassios, T. P., Yannopoulos, P. J. 1991. Reinforced concrete axial elements analyzed under monotonic and cyclic actions. *Aci Structural Journal* 88/1: 3-11.

Yang, S., Chen, J. 1988. Bond-slip and crack width calculations of tension members. *Aci Structural Journal* 85/4: 414-422.

Yankelevsky, D.Z. 1985. Bond action between concrete and a deformed bar - a new model. *Aci Journal* 85/1: 154-161